Tutorial

Rolf Wester*

Physical optics methods for laser and nonlinear optics simulations

Abstract: The development of optical systems today is strongly supported by computer simulations. Computer ray tracing tools are well established in the field of geometrical optics for designing objectives, light channels, etc. Ray tracing is conceptually quite simple, which makes the implementation as well as the interpretation of ray tracing results easy, although the design of high-quality lens systems remains a challenging task. In the field of wave optics, there are software tools as well, but they are still not as mature as the ray tracing tools. The main reason for this is that numerically solving partial differential equations is numerically more complex and not as intuitive as ray tracing. Besides simple wave propagation, the main field of use of the wave optics methods today is the development of lasers and laser resonator and nonlinear optics. The optical properties of the media, in general, depend on the temperature and mechanical stresses. The interaction of the electromagnetic fields with matter, thus, has to self-consistently include thermomechanical computations.

Keywords: laser beam characterization; laser resonators; nonlinear optics; physical optics.

OCIS codes: 140.3295; 140.3410; 190.0190; 260.0260.

***Corresponding author: Rolf Wester,** Fraunhofer Institute for Laser Technology ILT, Steinbachstr. 15, 52074 Aachen, Germany, e-mail: rolf.wester@ilt.fraunhofer.de

1 Modeling optical systems

1.1 Levels of modeling

Depending on the experimental situation, light shows wave-like or particle-like behavior. Many properties of light cannot be interpreted within the frame of classical electrodynamics. The theory that describes all experimental observations not only qualitatively but also quantitatively with surprising precision is quantum electrodynamics [1, 2]. Nevertheless, classical electrodynamics is very successful in dealing with light intensities that are well above the single-photon level.

Classical optics can be carried out on different levels of detail and physical rigor. Totally incoherent light can often satisfactorily be described by geometrical optics, and the propagation of laser light is quite well treated employing the classical Maxwell equations. But even when neglecting the quantum effects, the mathematical complexity of Maxwell equations in their general form is considerable. Further simplifications lead from the "fully vectorial" to the "semiclassical" and finally to the "scalar" theory of wave optics [3].

2 Electrodynamics

2.1 Maxwell's equations

Electrodynamics is governed by the Maxwell's equations [4]:

$$\vec{\nabla}\times E=-\frac{\partial B}{\partial t} \tag{1}$$

$$\vec{\nabla}\times H=\vec{j}+\frac{\partial D}{\partial t} \tag{2}$$

$$\vec{\nabla}\cdot D=\rho \tag{3}$$

$$\vec{\nabla}\cdot H=0 \tag{4}$$

E is the electric field, and D is the electric displacement field. The nomenclature of B and H is not consistent in literature. According to [5], B is called the magnetic flux density or magnetic induction, and H is the magnetic field strength or magnetic field intensity. Current density $\vec{j}$ and space charges ρ will be neglected in the following. The fields B and H and E and D, respectively are connected by the material relations:

$$B=\mu_0 H+\vec{M} \tag{5}$$

$$D=\varepsilon_0 E+P \tag{6}$$

μ_0 is the vacuum permeability, and ε_0 is the vacuum dielectric constant or vacuum electric permittivity. In optics, almost always, the magnetization $\vec{M}$ can be neglected. In the linear case, the polarization P is given by:

$$P=\varepsilon_0 \underline{\chi} E. \tag{7}$$

The electric susceptibility $\underline{\chi}$, in general, is a second-rank tensor that mathematically describes the anisotropic electrical properties of matter. In isotropic media, $\underline{\chi}$ reduces to a scalar. Inserting into Equation (6) yields in the linear isotropic case:

$$D=\varepsilon_0 \varepsilon E \tag{8}$$

$$\varepsilon=1+\chi \tag{9}$$

ε is the relative dielectric constant.

2.2 Complex quantities

Although the fields are real quantities, it is often convenient to use complex quantities in the computations. Time harmonic fields can be expressed as:

$$E(x,y,z,t)=A(x,y,z)\exp[-i\omega t]+A^*(x,y,z)\exp[i\omega t] \tag{10}$$

$A(x,y,z)$ is a complex field amplitude. Because the Maxwell equations are linear in the field quantities (when considering nonlinear interactions, special caution has to be taken), the Maxwell equations separate into a set of equations for the complex amplitudes and the conjugates of the complex amplitudes, respectively. It suffices to solve only the equations for the complex field amplitudes. When expressions containing products of field quantities are involved, like the Poynting vector [4]:

$$S=E\times H \tag{11}$$

the real expression Equation (10) has to be taken. If E and H are perpendicular to each other, the Poynting vector norm is given by:

$$|S|=E\cdot E\frac{n}{Z_0} \tag{12}$$

with the vacuum impedance $Z_0=\frac{1}{\sqrt{\mu_0\varepsilon_0}}$ and the index of refraction $n=\sqrt{\varepsilon}$. Using Equation (10) and integrating over a period of time T yields the intensity:

$$\begin{aligned} I=&\frac{2}{Z_0}\frac{1}{T}\int_t^{t+T} AA^* dt+\frac{1}{Z_0 T}\int_t^{t+T} AA\exp[-i2\omega t]dt \\ &+\frac{1}{Z_0 T}\int_t^{t+T} A^*A^*\exp[i2\omega t]dt. \end{aligned} \tag{13}$$

The second and third integrals vanish, thus:

$$I=\frac{2AA^*}{Z_0} \tag{14}$$

In the literature, the field E is sometimes defined as:

$$\begin{aligned} E(x,y,z,t)=&\frac{1}{2}\big(A(x,y,z)\exp[-i\omega t] \\ &+A^*(x,y,z)\exp[i\omega t]\big) \end{aligned} \tag{15}$$

The intensity, then, is given by:

$$I=\frac{AA^*}{2Z_0}. \tag{16}$$

2.3 Time-dependent nonlinear wave equation

The following time-dependent wave equation can be deduced from Maxwell's equations [6]:

$$\Delta E(\vec{r},t)-\vec{\nabla}\left(\vec{\nabla}\cdot E(\vec{r},t)\right)-\mu_0\frac{\partial^2 D(\vec{r},t)}{\partial t^2}=0. \tag{17}$$

The dielectric displacement field is determined by the electric field and, if not in the vacuum, by the response of the matter to the electric field. The response, in general, is not linear. Usually, $\vec{D}$ is expressed by a series of powers of $\vec{E}$. Including the linear and second-order terms, the displacement vector, $\vec{D}$, is given by:

$$D(\vec{r},t)=\varepsilon_0 E(\vec{r},t)+P_L(\vec{r},t)+P_{NL}(\vec{r},t) \tag{18}$$

with the linear response:

$$\vec{P}_L(\vec{r},t)=\varepsilon_0\int_{-\infty}^{\infty}\chi^{(1)}(\vec{r}_1,t_1)\cdot E(\vec{r}-\vec{r}_1,t-t_1)d\vec{r}_1 dt_1 \tag{19}$$

and the lowest-order nonlinear or second-order response [6]:

$$\begin{aligned} \vec{P}_{NL}(\vec{r},t)=&\varepsilon_0\int_{-\infty}^{\infty}\chi^{(2)}(\vec{r}_1,t_1;\vec{r}_2,t_2):E(\vec{r}-\vec{r}_1,t-t_1) \\ &E(\vec{r}-\vec{r}_2,t-t_2)d\vec{r}_1 dt_1 d\vec{r}_2 dt_2 \end{aligned} \tag{20}$$

$\chi^{(2)}$ is a rank-three tensor. The colon in the above equation denotes a tensor product. Using components, this reads:

$$\left(\chi^{(2)}:EE\right)_i=\sum_j\sum_k \chi_{ijk}^{(2)}E_j E_k \tag{21}$$

With this, the wave equation can be written as:

$$\Delta E(\vec{r},t)-\vec{\nabla}\left(\vec{\nabla}\cdot E(\vec{r},t)\right)-\mu_0\frac{\partial^2 D_L(\vec{r},t)}{\partial t^2}=\mu_0\frac{\partial^2 P_{NL}(\vec{r},t)}{\partial t^2}. \tag{22}$$

This is the 'full-vectorial' wave equation governing the propagation of electromagnetic fields up to the second order in the polarization. In general, the second term on the left-hand side couples all the electric field components. Neglecting those parts of this term that couple the electric field components yields the 'semivectorial' theory, and neglecting this term entirely yields the 'scalar' theory. Neglecting the coupling term and the nonlinear polarization on the right-hand side of Equation (22) and assuming the harmonic time dependence $\exp(-i\omega t)$ leads to the much simpler time-independent scalar Helmholtz equation:

$$\Delta E(\vec{r},\omega)+n^2k_0^2E(\vec{r},\omega)=0 \tag{23}$$

with the index of refraction $n=\sqrt{\varepsilon}$, the vacuum wave number $k_0=\frac{\omega}{c_0}$ and the vacuum velocity of light $c_0=1/\sqrt{\mu_0\varepsilon_0}$.

2.4 Solutions of the Helmholtz wave equation

Solutions of the Helmholtz wave equation, Equation (23), can be expressed by the angular spectrum representation [7]:

$$E(x,y,z)=\int_{-\infty}^{\infty}\int_{-\infty}^{\infty}\hat{E}(k_x,k_y;z=0)\exp\left(i\sqrt{k_0^2-k_x^2-k_y^2}z\right)\exp\left(i(k_xx+k_yy)\right)\mathrm{d}k_x\,\mathrm{d}k_y \tag{24}$$

with:

$$\hat{E}(k_x,k_y;z=0)=\int_{-\infty}^{\infty}\int_{-\infty}^{\infty}E(x',y';z=0)\exp\left(-i(k_xx'+k_yy')\right)\mathrm{d}x'\,\mathrm{d}y'$$

$E(x',y';z=0)$ is the field at the plane at $z=0$, and $E(x,y,z)$ is the field at the plane at $z>0$. k_x and k_y are the spatial frequency components. The function values of $\hat{E}(k_x,k_y)$ with $k_x^2+k_y^2<k_0^2$ are the amplitudes of propagating modes, whereas the amplitudes with $k_x^2+k_y^2\geq k_0^2$ correspond to the evanescent waves. The field propagation expressed by Equation (24) is exact within the frame of scalar wave theory. The angular spectrum representation is equivalent to the Rayleigh-Sommerfeld diffraction formulae [8]. The paraxial approximation $k_x=k_0$, $k_y=k_0$:

$$\sqrt{k_0^2-k_x^2-k_y^2}\approx k_0-2\frac{k_x^2}{k_0}-2\frac{k_y^2}{k_0} \tag{25}$$

yields the Fresnel diffraction integral [9]:

$$E(x,y,z)=\exp(ik_0z)\int_{-\infty}^{\infty}\int_{-\infty}^{\infty}\hat{E}(k_x,k_y;z=0)\exp\left(-i\frac{\lambda}{\pi}\left(k_x^2+k_y^2\right)z\right)\exp\left(i(k_xx+k_yy)\right)\mathrm{d}k_x\,\mathrm{d}k_y \tag{26}$$

Equation (26) is equivalent to a convolution in position space, the way the Fresnel diffraction integral usually is expressed.

2.5 One-way wave equation and slowly varying envelope approximation

In many cases of interest, Maxwell's equations, or thereof reduced wave equations, cannot be solved analytically, but numerical methods have to be employed. In homogeneous media, solutions to the Helmholtz equation are given by the angular spectrum representation, and the propagation of fields can easily be computed using Fourier transformations. In the case of inhomogeneous media like wave guides or fiber, different approaches can be employed:

- Discretize Maxwell's equations in time and space resolving the wavelength and time period (finite difference time domain method), which results in an initial-boundary-value problem.
- Separating out fast-oscillating factors yielding one-way wave equations that can be integrated along the propagation direction with suitable initial conditions.

The first approach is more exact but is computationally very demanding and is not suitable for domains much larger than the wavelength. The second one reduces in the simplest case to the slowly varying envelope (SVE) approximation. With the Helmholtz equation:

$$\frac{\partial^2E}{\partial x^2}+\frac{\partial^2E}{\partial y^2}+\frac{\partial^2E}{\partial z^2}+n^2k_0^2E=0 \tag{27}$$

and separating out the fast-oscillating part:

$$E(x,y,z)=E_0(x,y,z)\exp\left(-in_0k_0z\right) \tag{28}$$

yields the so-called one-way wave equation [10]:

$$\frac{\partial}{\partial z}\left(2in_0k_0-\frac{\partial}{\partial z}\right)E_0=PE_0 \tag{29}$$

$$P=\frac{\partial^2}{\partial x^2}+\frac{\partial^2}{\partial y^2}+\left(n^2-n_0^2\right)k_0^2. \tag{30}$$

Neglecting $\frac{\partial}{\partial z}$ compared to $2in_0k_0$ on the right-hand side yields the SVE approximation. The SVE approximation is limited to field components with the wave vectors close to parallel to the main propagation direction. Higher-order or wide-angle approximations can be constructed by the recursion:

$$\frac{\partial}{\partial z}|_{i+1}=\frac{P}{2in_0k_0-\frac{\partial}{\partial z}|_i} \tag{31}$$

which yields higher Padé approximants of the propagation operator [10, 11]. Figure 1 shows the intensity profile of an initially Super-Gaussian after propagating a distance, L.

2.6 Nonlinear three-wave mixing

Nonlinear three-wave mixing is an established means for producing monochromatic coherent light at wavelengths not or not easily creatable by other means. Efficient green coherent light sources can be realized by frequency doubling of solid state laser beams at, e.g., 1060 nm (Nd:YAG). In the lowest-order nonlinear processes, in general, three different wavelengths are involved. The modeling, thus, needs to solve three-wave equations with nonlinear coupling terms. The wave equations can be deduced from the general wave equation [Equation (7)] and the nonlinear polarization PNL. In the SVE approximation, the wave equations for three-wave mixing read [6]:

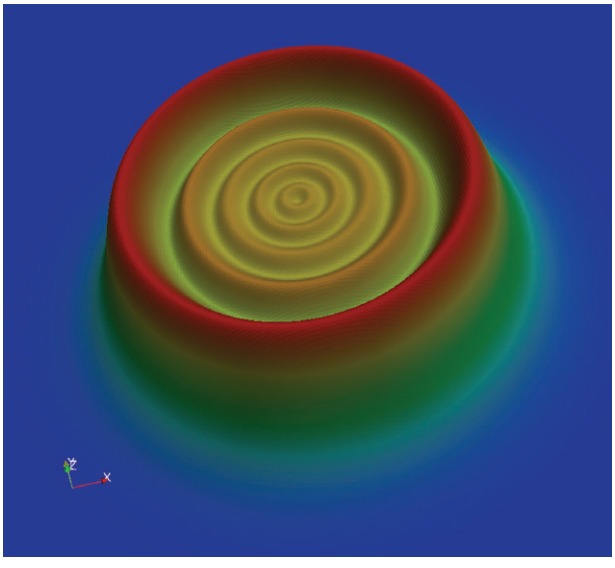

Figure 1 The intensity profile of an initially super Gaussian with beam radius, w_0, after a propagation distance of $L\approx\frac{w_0^2}{10\lambda}$.

$$\frac{\partial E_s(\vec{r},t)}{\partial z}=\Delta_t E_s+\alpha_s E_s+k_{0s}^2\left(n_s^2-n_s^2\right)+\frac{i2d_{eff}k_{0s}}{n_s}E_pE_i^*\exp(-i\Delta kz) \tag{32}$$

$$\frac{\partial E_i(\vec{r},t)}{\partial z}=\Delta_t E_i+\alpha_i E_i+k_{0i}^2\left(n_i^2-n_i^2\right)+\frac{i2d_{eff}k_{0i}}{n_i}E_pE_s^*\exp(-i\Delta kz) \tag{33}$$

$$\frac{\partial E_p(\vec{r},t)}{\partial z}=\Delta_t E_p+\alpha_p E_p+k_{0p}^2\left(n_p^2-n_p^2\right)+\frac{i2d_{eff}k_{0p}}{n_p}E_sE_i\exp(i\Delta kz) \tag{34}$$

$$\Delta k=k_{0s}n_s+k_{0i}n_i-k_{0p}n_p \tag{35}$$

$$\Delta_t=\frac{\partial^2}{\partial x^2}+\frac{\partial^2}{\partial y^2}. \tag{36}$$

The indices s,i,p designate the signal, idler, and pump waves, respectively. The α_j are the absorption coefficients that depend on the wavelengths of the wave. In general, the absorption increases with decreasing wavelength. d_{eff} is the effective coupling coefficient that not only depends on the nonlinear material but also on the field polarization.

The phase mismatch (Δkz) depends on the refractive indices of the three waves. The refractive indices depend on the wavelength and the field polarization. For efficient energy transfer, the phase mismatch at the end of the crystal (ΔkL) has to be smaller than π, with the crystal length, L. In the case of frequency doubling, the wavelengths and refractive indices of the signal and idler waves, respectively, are equal, i.e., $k_{0s}=k_{0i}$ and $n_s=n_i$, so that the phase mismatch is given by $\Delta kL=k_{0s}(2n_s-2n_p)L$. The refractive index difference n_s-n_p, thus, has to be smaller than $\lambda/4L$. With the typical values λ=1 μm and L=20 mm, this means $\Delta n<10^{-5}$. When considering only a single polarization direction, the refractive index difference at the two wavelengths λ_s and $\lambda_p=\lambda_s/2$ is much larger than this value. But choosing the different polarizations for the pump and signal waves, respectively, makes phase matching possible. The refractive indices also depend on the temperature and thermal-induced stresses. The phase-matching temperature acceptance depends on the material at hand. The typical values range from a few Kcm up to tens of Kcm , so depending on the crystal used, thermal management is crucial.

In the case of very short pulses, the three waves do not have single frequencies any more but a continuous spectrum given by the Fourier transform of the temporal

pulse shape [12]. In that case, the dispersion effects such as group velocity differences and group velocity dispersion have to be accounted for in the modeling. Figure 2 shows, as an example, the intensity change of the fundamental and the second harmonic wave during frequency doubling within the nonlinear crystal. The asymmetry of the intensity of the converted wave with respect to the optical axis is due to the walk-off, which is caused by birefringence.

3 Optical elements

Free space propagation of light fields is a special case of the more general case of propagation in a dispersive, inhomogeneous, anisotropic, absorbing, or amplifying medium. The numerical methods for solving this general problem in the case of optical wavelengths and macroscopic optical systems very often employ some kind of approximation. Operator splitting is, in many cases, used to separate diffraction and interactions between the light field and the medium, as e.g., refraction at index interfaces, amplification, birefringence, and nonlinear wave mixing. That means diffraction is computed along the propagation length, L, neglecting the other processes, and subsequently, the same step is repeated, neglecting diffraction but taking into account one of the other relevant processes.

3.1 Paraxial beams and optical elements

Laser light is distinguished by its high beam quality, which makes possible the laser beams with small divergence angles. If the paraxial approximation can be used, the nondiffracting processes can often be modeled by thin sheets; e.g., thin lenses and mirrors can be modeled by multiplications of the field by a phase factor:

$$E_{out}(x,y,z)=\exp(-ik\phi(x,y))E_{in}(x,y,z) \tag{37}$$

with:

$$\phi(x,y)=\frac{x^2+y^2}{2f} \tag{38}$$

for lenses and:

$$\phi(x,y)=\frac{x^2+y^2}{R} \tag{39}$$

in case of mirrors with f the focal length of the lens and R the radius of curvature of the mirror. As the above equations indicate, the field E_{out} at the point (x,y,z) only depends on the input field E_{in} at the same point. In the case of the paraxial beams and thin optical elements, the ABCD matrix formalism can be used to model the propagation through the optical system including the diffraction using Collins from of the Fresnel diffraction integral [13].

3.2 Gain media

The intensity change in a gain medium can be expressed by the light transfer equation, which in the one-dimensional case is given by [14]:

$$\frac{dI(x,y)}{dz}=g(x,y)I(x,y). \tag{40}$$

Owing to the saturation, the gain coefficient, $g(x,y)$, in general, depends on the field intensity, and thus, Equation (40) is nonlinear.

3.2.1 Stationary homogeneously broadened media

The steady-state gain coefficient of the homogeneously broadened media is given by the expression [15]:

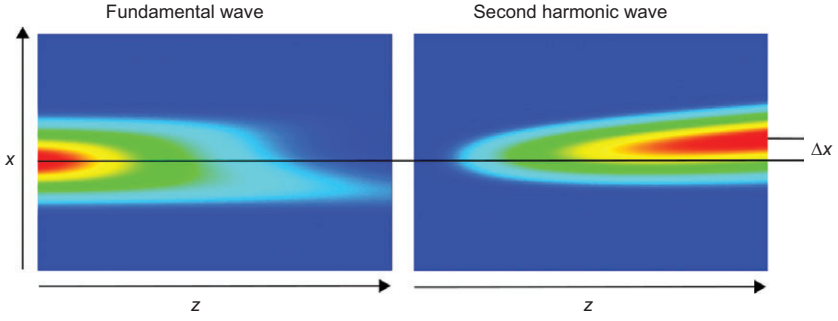

Figure 2 Simulation of the second-harmonic generation. The displacement Δx of the center of the intensity distribution of the second harmonic is called the walk-off. The walk-off is a result of the wave vector and the Poynting vector not being parallel in the anisotropic material [9].

$$g(x,y)=\frac{g_0(x,y)}{1+\frac{I(x,y)}{I_s(x,y)}} \tag{41}$$

g_0 is the small-signal gain coefficient, which depends on the pump rate and the active laser system at hand. I is the radiation intensity, and I_s is the saturation intensity. I_s is mainly determined by the ratio of the spontaneous emission rate and transition rates between the upper laser level and the other levels that do not contribute to the laser activity (e.g., nonradiative transitions). When the intensity equals the saturation intensity, the gain coefficient amounts to half of the small-signal gain value. The input and output fields are connected by:

$$E_{out}(x,y,z)=E_{in}(x,y,z+L)\exp\left(\frac{1}{2}g(x,y,I(x,y))L\right) \tag{42}$$

with a suitable average of $g(x,y;I(x,y))$ between z and $z+L$.

3.2.2 Pulsed gain

The gain of transiently pumped laser media can be determined by solving the time-dependent rate equations for the relevant laser levels and the radiation field.

3.3 Thick lenses

In the case of the thick lenses, things are more involved. The pointwise connection between the input and output fields is not valid any more if Δx in Figure 3 cannot be assumed to be small. The numerical simulation of wave propagation through the index interfaces of curved surfaces is not easily done. The two most popular methods to circumvent this problem are:

1. Coherent decomposition of the light field into Gaussian beamlets and propagating the Gaussians using the methods presented in [16].
2. If the propagation distance through the thick lens is sufficiently short so that the geometric optics is valid at least approximately, the propagation can be implemented by ray tracing. The ray directions in the input plane are given by the normals of the surfaces of constant phase. Summing the optical path lengths while tracing the rays through the lens yields the phase in the output plane. The ray coordinates are transformed to the output plane. The Jacobian of this transformation can be used to compute the intensity and the light field in the output plane using the radiant power on the area elements in the input plane.

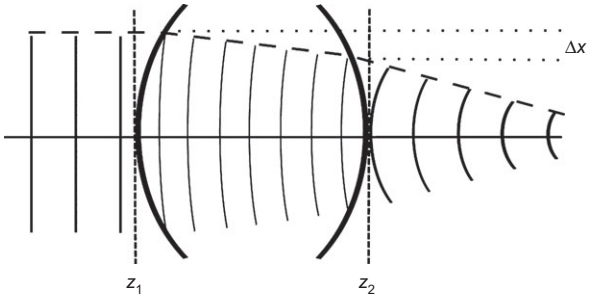

Figure 3 Thick convex-convex lens. A plane wave is transformed into a spherical wave. The transversal beam extend changes during propagation from the input plane at z_1 to the output plane at z_2 by Δx.

4 Thermally induced optical effects

The numerical modeling of propagation in the homogeneous media, of the paraxial first-order quadratic index elements, of the thick lenses via geometric optics, and so on are well established techniques in optics simulations. Things get more complicated when the optical fields change the optical properties by absorption and heating of the optical components. The refractive indices of most materials depend on the temperature and on the mechanical state, i.e., internal stresses. The internal stresses are not only induced by the external forces but also by the inhomogeneous temperature distributions. Even the isotropic materials, in general, become birefringent when internal stresses are present. The refractive index, thus, depends on the position and on the polarization of the radiation. The wave equation, Equation (22), describes all this phenomena. But a general solution is hard to achieve. In many cases of interest, it suffices to split the propagation through the inhomogeneous medium into small-enough steps so that the impact of the inhomogeneity and anisotropy can be described by thin sheets. Diffraction again can be handled by operator splitting.

4.1 Jones matrices

Mathematically, the thin sheets coupling the field polarization components can be described by the Jones matrices. The electric field and the dielectric displacement are related by the dielectric tensor ε or the inverse dielectric tensor B:

$$\vec{D}=\varepsilon_0\varepsilon\vec{E} \tag{43}$$

$$\vec{E}=\frac{1}{\varepsilon_0}B\vec{D}. \tag{44}$$

In the linear material response limit, the contributions of the temperature and mechanical stresses to B can be separated according to:

$$B(T,\varepsilon_M)=B_T(T)+B_M(\varepsilon_M) \tag{45}$$

ε_M in this equation is the mechanical strain tensor and must not be confused with the dielectric constant. The temperature-dependent part is given in the principal axis system by:

$$B_T^{(p)}=\begin{pmatrix} \frac{1}{n_1^2(T)} & 0 & 0 \\ 0 & \frac{1}{n_2^2(T)} & 0 \\ 0 & 0 & \frac{1}{n_3^2(T)} \end{pmatrix} \tag{46}$$

$n_i(T)$ is the temperature-dependent index of refraction of the *i'th* polarization direction. The Taylor series expansion yields:

$$n_i(T)=n_i|_{T_0}+\frac{dn_i}{dT}|_{T_0}(T\text{-}T_0)+\frac{1}{2}\frac{d^2n_i}{dT^2}|_{T_0}(T\text{-}T_0)^2+\ldots \tag{47}$$

In many cases, the linear factor $\frac{dn_i}{dT}$ suffices. The tensor Equation (46) has to be transformed into the optical axis system.

The part, depending on the mechanical strain, is a linear function of the strain components:

$$B_{M;ij}(\varepsilon)=\sum_{k=1}^{3}\sum_{l=1}^{3}p_{ijkl}\varepsilon_{M;kl} \tag{48}$$

p_{ijkl} is the photoelastic tensor of rank 4, and $\varepsilon_{M;kl}$ are the components of the second-rank strain tensor. T and $\varepsilon_{M;kl}$ have to be computed, e.g., using a FEM program with the deposited power density calculated from radiation absorption. Because the propagation of light fields depends on the refractive index, this has to be done self-consistently.

The tensor, B, is projected onto the x-y plane of the optical axis system. The resulting two-dimensional tensor B_{red} is transformed into its principal axis system. The field components in the principal axis system E_1 and E_2 are propagated according to:

$$\begin{pmatrix} E_1(z) \\ E_2(z) \end{pmatrix}=\begin{pmatrix} \exp(-in_1k) & 0 \\ 0 & \exp(-in_2k) \end{pmatrix}\begin{pmatrix} E_1(0) \\ E_2(0) \end{pmatrix} \tag{49}$$

n_1 and n_2 are the eigenvalues of B_{red}. Transforming Equation (49) back into the laboratory frame yields:

$$\begin{pmatrix} E_x^{(2)}(x,y) \\ E_y^{(2)}(x,y) \end{pmatrix}=\begin{pmatrix} J_{xx}(x,y) & J_{xy}(x,y) \\ J_{xy}(x,y) & J_{yy}(x,y) \end{pmatrix}\begin{pmatrix} E_x^{(1)}(x,y) \\ E_y^{(1)}(x,y) \end{pmatrix}. \tag{50}$$

This is the paraxial Jones matrix model. The field components are coupled and multiplied by spatially dependent phase factors. This includes thermal lens effects. Besides thermal lensing polarization losses are a significant problem in solid state lasers. The polarization losses mean that when starting with a field that only has an x-component, after propagating through the laser medium, part of the x-component power is transferred to the y-component [17]. Figure 4 shows the polarization loss of a homogeneously heated Nd:YAG laser rod.

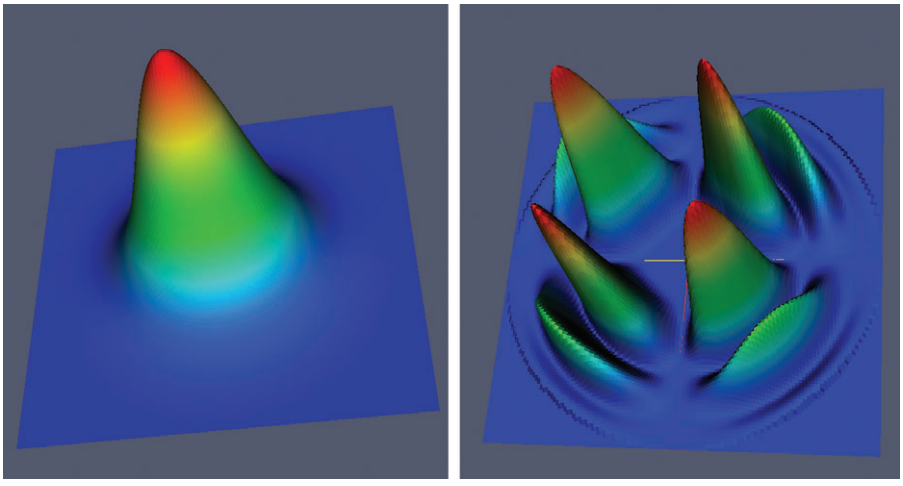

Figure 4 Left: intensity of the x-component of a Gaussian before propagating through a homogeneously heated Nd:YAG rod. Right: intensity of the y-component after propagating through the rod showing birefringence (The scales on the left and right sides are different.).

5 Summary

Physical optics modeling and numerical simulation is of great usefulness for better understanding the behavior of complex optical systems and for improving performance of, e.g., lasers, especially solid state lasers, and nonlinear frequency conversion. The models and numerical methods have to be sufficiently accurate but also efficient. The vectorial descriptions of light can often be reduced to scalar models, which makes, e.g., the treatment of diffraction much easier. When the vector character cannot be neglected, like in birefringent materials, the mathematical model often can be reduced to two uncoupled propagation equations for two scalar field components that are coupled by applying the Jones matrices. Thermal lensing, temperature dependence of refractive indices, and temperature-induced mechanical stresses that change the optical properties make necessary a self-consistent treatment of optics and thermomechanics.

All the models and methods described in the present article are implemented in a numerical package [18] and proofed their usefulness in the development of many real-world optical systems in the field of solid state lasers [17] and nonlinear frequency conversion [19–25]. The development of the software package has not been a one-way road, but feedback from the experiments helped to improve its correctness and reliability.

Received October 5, 2012; accepted January 18, 2013; previously published online March 14, 2013

References

[1] R. P. Feynman, in 'Quantum Electrodynamics' (Westview Press, Boulder Colorado, 1989).
[2] W. Greiner, in 'Quantum Electrodynamics' (Springer, Berlin, Heidelberg, 2008).
[3] C. L. Xu and W. P. Huang, in 'Progress in Electromagnetics Research, Electromagnetic Waves, PIER 11' (EWM Publishing Cambridge, 1995) pp. 1–49.
[4] J. D. Jackson, in 'Classical Electrodynamics' (John Wiley & Sons, New York, Chichester, Weinheim, Brisbane, Singapore, Toronto, 1998).
[5] E. J. Rothwell and M. J. Cloud, in 'Electromagnetics' (CRC Press, Boca Raton) p. 23.
[6] R. W. Boyd, in 'Nonlinear Optics' (Academic Press, Burlington, San Diego, 2008).
[7] L. Mandel and E. Wolf, in 'Optical Coherence and Quantum Optics' (Cambridge University Press, Cambridge, New York, 1995).
[8] P. Liu and B. Lü, Opt. Laser Technol. 39.4, 741–744 (2007).
[9] M. Born, E. Wolf, A. B. Bhatia, P. C. Clemmow, D. Gabor, et al. in 'Principles of Optics: Electromagnetic Theory of Propagation, Interference and Diffraction of Light' (Pergamon Press, Oxford, 1999).
[10] S. L. Chui and Y. Y. Lu, J. Opt. Soc. Am. A 21.3, 420–425 (2004).
[11] G. R. Hadley, Opt. Lett. 17, 1426–1428 (1992).
[12] T. Brabec and F. Krausz, Phys. Rev. Lett. 78, 3282 (1997).
[13] S. A. Collins, J. Opt. Soc. Am. 60, 1168–1177 (1970).
[14] J. Cannon, in 'The Transfer of Spectral Line Radiation' (Cambridge University Press, Cambridge, New York, Melbourne, Madrid, Cape Town, Singapore, Sao Paulo, Delhi, Tokyo, Mexico City, 1985).
[15] W. Kleen and R. Müller, in 'Laser' (Springer, Berlin, 1969).
[16] J. Arnaud. Appl. Opt. 24, 538–543 (1985).
[17] G. Schmidt, R. Wester, H.-D. Hoffmann, G. Bonati, P. Loosen, et al. in 'Proc. of the SPIE 3613, Solid State Lasers VIII', Vol. 3613 (1999).
[18] R. Wester, M. Höfer and B. Gronloh, in 'OPT – Physical optics software package for simulating lasers and non-linear optical systems including thermo-mechanical effects' (Copyright: Fraunhofer Institut Lasertechnik, Aachen, 1998–2012).
[19] B. Gronloh, M. Höfer, R.Wester and H.-D. Hoffmann, in 'Proc. of the SPIE, Solid State Lasers XVIII: Technology and Devices', Vol. 7193 (San Jose, 2009) p. 71930Y-1.
[20] B. Gronloh, T. Mans, P. Rußbüldt, B. Jungbluth, R. Wester and D. Hoffmann, in 'Advanced Solid-State Photonics', OSA Technical Digest Series (CD) (Optical Society of America, 2010), paper ATuA13.
[21] B. Gronloh, P. Russbueldt, W. Schneider, B. Jungbluth and H.-D. Hoffmann, in 'Proc. of the SPIE, Solid State Lasers XXI: Technology and Devices', Vol. 8235 (2012) p. 82351C.
[22] B. J. und Sebastian Nyga und Enno Pawlowski und Thomas Fink und Jochen Wueppen, in 'Proc. of the SPIE., Solid State Lasers XX: Technology and Devices', Vol. 7912 (2011) p. 79120K.
[23] S. N. und Jens Geiger und Bernd Jungbluth, in 'Proc. of the SPIE., Solid State Lasers XIX: Technology and Devices', Vol. 7578 (2010) p. 75780P.
[24] J. Wueppen, B. Jungbluth, J. Geiger, D. Hoffmann and R. Poprawe, in 'Advanced Solid-State Photonics', OSA/ASSP (2005) p. TUB23.
[25] J. Wueppen, E. Pawlowski, M. Traub, B. Jungbluth, K.-H. Hasler, et al. in 'Proc. of the SPIE., Nonlinear Frequency Generation Applications IX', Vol. 7582 (2010) p. 758204.

Rolf Wester is a scientist at the Fraunhofer ILT in Aachen. He received his Diploma (MSc) in Physics in 1983 from the Technical University of Darmstadt and his Doctorate (PhD) in 1987 from the RWTH Aachen. In the same year he changed from the RWTH to the Fraunhofer ILT where he continued working on high frequency excitation of gas lasers. In recent years his fields of research interests switched to optics. He is now mainly concerned with the development of simulation software for physical optics problems and of numerical design tools for freeform optical elements.